ELSEVIER

Journal of Nuclear Materials 281 (2000) 195–202

journal of nuclear materials

www.elsevier.nl/locate/jnucmat

Dynamic behaviour of the systems Be–C, Be–W and C–W

W. Eckstein *

Max-Planck-Institut für Plasmaphysik, Boltzmannstrasse 2, D-85748, Garching bei München, Germany

Received 7 April 2000; accepted 9 June 2000

Abstract

The Monte Carlo program TRIDYN is applied to investigate the dynamic behaviour of the binary systems Be–C, Be–W and C–W, where one species represents the bombarding atom and the other the target atom. The fluence dependence of the particle reflection coefficient, of the sputtering yield, of the target composition, and of implantation values is calculated for incident energies between 300 eV and 10 keV (in a few cases up to 1 MeV) and for various angles of incidence. © 2000 Elsevier Science B.V. All rights reserved.

1. Introduction

In contrast to ion bombardment studies with gaseous ions, mainly noble gas ions, this paper deals with incident projectiles which form solids at room temperature. These projectiles can build up solid layers inside or on top of the bombarded target which is, in general, possible for gaseous ions only at very low temperatures or if the ions form compounds with target atoms. Although bombardments with ions forming solids have been performed in the field of doping semiconductors as Si with B or P, for example, the incident fluences were usually rather low to produce only low concentrations of these dopants in the target. Higher fluxes than those in ion beams are achieved in plasmas which allow also higher fluences. In today's fusion plasma devices the most common first wall materials are low Z (atomic number) elements such as C and Be as well as B in the form of thin films. In the design of a future large fusion machine, ITER [1], three elements, Be, C and W, are proposed to be implemented in the machine at different locations. Besides the bombardment with hydrogen isotopes, the walls of the main vessel and divertors are bombarded with ions (or atoms) from all material species existing in the machine. Material mixing in fusion devices has been observed [2–4]. However, it seems reasonable to study simple binary systems first.

Previous investigations of the bombardment of W by C for incident energies of 1 and 6 keV have shown [5], that at an angle of incidence of about 40° (with respect to the surface normal) the deposition behaviour at small angles of incidence changes into an erosion behaviour at large angles of incidence under steady-state conditions. Calculated values agreed reasonably well with experimental data of the weight change. Similar results have been found in [6] for the bombardment of Be with 3 keV C.

The present calculations with TRIDYN extend the earlier studies to a larger energy range and to the inverse systems, bombardment of Be, C and W with W, C and Be, respectively.

2. The simulation code

The calculations have been performed with the Monte Carlo program TRIDYN (version 40.3) [7,8], which is based on TRIM.SP [8,9]. It is a Monte Carlo program which assumes a randomized target structure and treats the atomic interactions as a sequence of binary collisions between atoms. In all calculations the WHB (Kr–C) potential [10] is applied. For the electronic energy loss an equipartition of Lindhard and Scharff [11] and Oen and Robinson [12] models is used. TRIDYN takes target composition changes by collisional effects into account and allows to determine sputtering yields, reflection coefficients, and several other bombardment related effects as a function of the incident fluence.

* Tel.: +49-8932 991 259; fax: +49-8932 991 499.
E-mail address: wge@ipp.mpg.de (W. Eckstein).

0022-3115/00/$ - see front matter © 2000 Elsevier Science B.V. All rights reserved.
PII: S0022-3115(00)00189-6

A projectile and the recoils generated by it are followed from collision to collision until their energy is below a threshold energy (typically the surface binding energy). After each projectile and all its recoil atoms have come to rest the depth distribution of the elemental composition and the density are updated. The density is calculated by the reciprocal addition of the atomic densities of the pure elements according to the composition [7,8]. The surface binding energy is varied between the heat of sublimation for the pure elements and the mean value of both numbers (model 3 in [13]). Diffusion and/or segregation is not taken into account which seems to be justified at room temperature or below for the systems investigated, which is inferred from the good agreement with an earlier comparison of experimental and calculated values [5]. The available diffusion coefficients of C in W imply a negligible diffusion below 700 K [14].

The calculations have been performed for the bombardment of Be with C and W, C with Be and W, and W with Be and C in the energy range from 0.1 to 10 keV in most instances, with few calculations up to 1 MeV, and for various angles of incidence.

3. Results and discussion

It is worthwhile to clarify the terminology in this paper. During all ion bombardments three processes occur: backscattering, sputtering and implantation. Only at energies below the sputtering threshold, sputtering is not possible, and for very low target mass to ion mass ratios backscattering becomes extremely improbable. Due to implantation of the incident species the originally pure elemental target turns to a two component target with a depth dependent composition in the implantation range. Steady-state or equilibrium is defined here by the situation, that the reflection coefficients and the partial sputtering yields do not change anymore with increasing fluence. If at steady-state the thickness of the target decreases with increasing fluence, the system is erosion dominated (shortly called erosion), though all three processes mentioned above are still at work. In the opposite case, where at steady-state the target thickness increases with increasing fluence, the system is deposition dominated (shortly called deposition).

If an energetic projectile hits a target it can be either implanted or backscattered (or transmitted, if the target is thin enough). In addition, energy is transferred in collisions to the target atoms which can eventually leave the target, i.e., sputtering. Implantation changes the target composition in the depth region, where the projectiles are stopped. This in turn changes the density of the target and the nuclear and electronic stopping of projectiles and recoils in that region. As a consequence, backscattering is changed; it will increase if the implanted species has a higher mass than the target species and vice versa. If the implanted species extends to the surface, the surface binding energy is changed according to the surface composition, which causes a change in the (partial) sputtering yields. Furthermore, the surface position is receding or growing according to the situation if more atoms are removed than implanted or vice versa. Finally, all these changes occur until steady-state conditions are reached. Naturally, all these effects depend on the incident energy, E_0, and on the incidence angle, α, of the projectile and on the target and projectile species.

As examples, the depth profiles of Be implanted into C at an incident energy of 500 eV and $\alpha = 40°$ and 50° (with respect to the surface normal) are shown in Fig. 1 for several incident fluences. The depth value of zero indicates the original surface position, the vertical lines show the actual surface position after some fluence. As can be seen in Fig. 1(a) for $\alpha = 40°$, the Be depth profiles become broader (extension to negative values) until

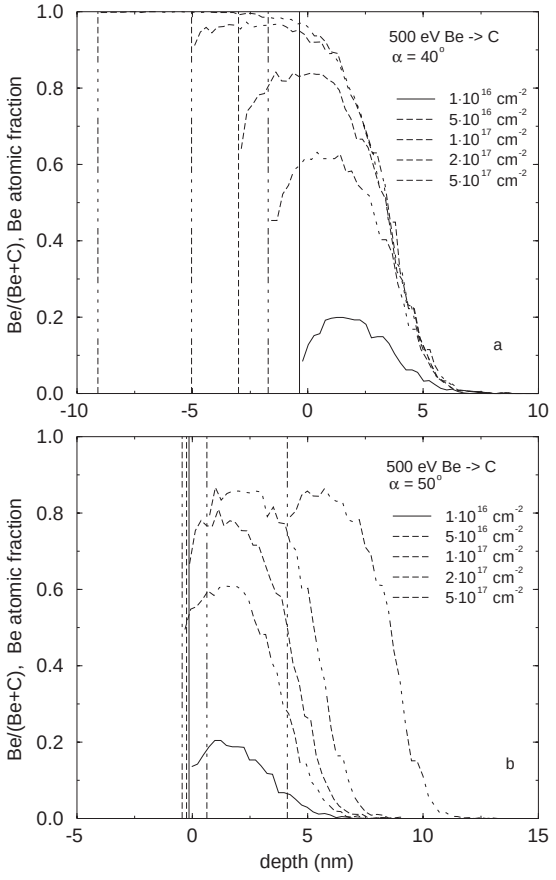

Fig. 1. Depth distribution of Be at several fluences for the bombardment of C with 500 eV Be at two angles of incidence (with respect to the surface normal): (a) $\alpha = 40°$ and (b) 50°.

steady-state is reached at a fluence of some 10^{17} atoms/cm^2 and a pure Be layer is formed. This means, that at steady-state the system is determined by Be self-sputtering and that the Be layer grows at a constant rate because the self-sputtering yield of Be is below unity. For $\alpha = 50°$ the target thickness initially increases slightly with the incident fluence until the surface recedes (move of the vertical lines to positive values), at fluences above 1×10^{17} atoms/cm^2 as shown in Fig. 1(b). The Be atomic fraction never reaches unity and, above some fluence ($\approx 1.5 \times 10^{17}$ atoms/cm^2), the Be depth profile gets constant and the surface recedes at a constant rate, steady-state is reached.

The surface movement is positive for an increasing and negative for a decreasing target thickness. The change of the target thickness with the incident fluence becomes constant at steady-state. It is positive for deposition and negative for erosion. The most rapid increase in the positive target thickness change occurs at normal incidence, and the largest negative target thickness change happens to be at about $\alpha = 70°$ for 500 eV Be impact on C. At an angle of incidence, $\alpha = 45°$, the target thickness change is positive for low fluences, but then it turns to a negative target thickness change. Therefore, the transition from deposition to erosion at steady-state occurs at an angle of incidence slightly smaller than $\alpha = 45°$. Close to the transition angle the fluences needed to reach steady-state conditions become rather large. The mean depth of the Be layer increases linearly with the Be fluence at steady-state in the deposition case, whereas it becomes constant in the erosion regime.

The number of implanted atoms is $N * (1 - R_N)$, where N is the number of incident projectiles, and R_N is the particle reflection coefficient. The number of atoms removed from the target is given by the sum of the partial sputtering yields, $N * \sum Y_i$, where i denotes the different species in the target including the projectile species. In the case discussed here, C is the only target species at the beginning of the implantation (zero fluence), but after some fluence the target contains also the projectile species which is Be. If $1 - R_N > \sum Y_i$, then the number of implanted atoms is larger than the number of atoms removed from the target, and deposition occurs. In the opposite case, $1 - R_N < \sum Y_i$, erosion dominates. It may happen, that a deposition behaviour changes into an erosion situation with increasing fluence or the opposite behaviour may occur. At steady-state, the partial sputtering yields of the (original) target species must become zero in the deposition case. The condition for the change of a deposition into an erosion regime is given by the equality of implanted and sputtered atoms, namely, the number of the implanted species, $(1 - R_N)$ equals the number of sputtered species, $(Y_{Be} + Y_C)$:

$$1 - R_N = Y_{Be} + Y_C = Y_{tot}. \quad (1)$$

This is demonstrated for 500 eV Be bombardment of C at $\alpha = 40°$ and 50°, for which R_N, Y_{Be}, Y_C, and Y_{tot} is shown in Fig. 2(a) and (b) versus the incident fluence. In both cases the Be sputtering yield increases with increasing fluence over the sputtering yields of C, but for $\alpha = 40°$ the sputtering yield of C gets zero for larger fluences which is not the case for $\alpha = 50°$. This result is obvious from the Be depth profiles in Fig. 1. The change of the particle reflection coefficients is small in both cases due to the small mass difference of Be and C. The horizontal line gives the condition $R_N + Y_{tot} = 1$ which separates the deposition and erosion regime. The case of $\alpha = 40°$ is clearly in the deposition regime, whereas the case of $\alpha = 50°$ is in the erosion regime. The fluctuations seen in Fig. 2 are of statistical origin.

Plotting $R_N + Y_{tot}$ versus the angle of incidence, α, at steady-state conditions clearly determines the angle of incidence region for deposition and erosion, see Fig. 3.

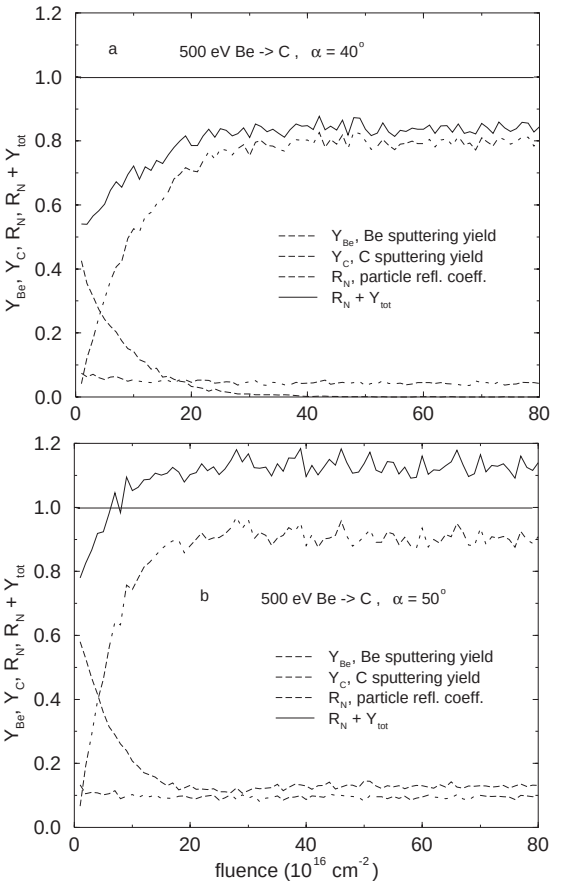

Fig. 2. Partial sputtering yields, Y_{Be} and Y_C, particle reflection coefficient, R_N, total sputtering yield, $Y_{tot} = Y_{Be} + Y_C$, and $R_N + Y_{tot}$ versus the fluence of 500 eV Be on a C target at an angle of incidence (with respect to the surface normal) of (a) 40° and (b) 50°.

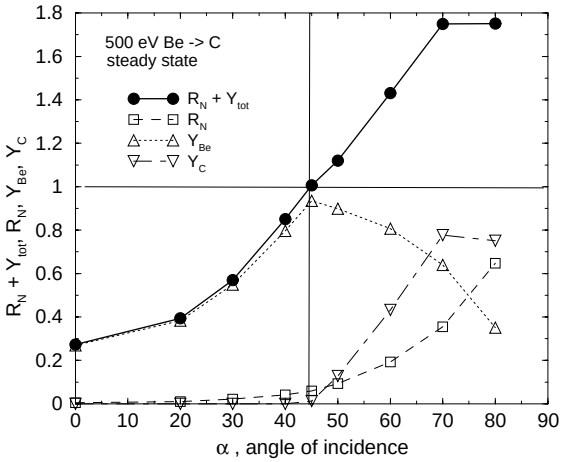

Fig. 3. $R_N + Y_{\text{tot}}$ versus the angle of incidence, α, at steady-state for the bombardment of C with 500 eV Be. Line drawn to guide the eye.

The condition $R_N + Y_{\text{tot}} < 1$ defines the deposition regime and the condition $R_N + Y_{\text{tot}} > 1$ the erosion regime. In the example of 500 eV Be bombardment of C the transition point is close to $\alpha = 40°$. The point at $\alpha = 45°$ is slightly above the unity line, which explains why the partial C sputtering yield is not equal to zero, see Fig. 4. For angles of incidence $\alpha < 45°$ the Be sputtering yield dominates the behaviour, whereas at angles $\alpha > 45°$ R_N and Y_{C} increase and Y_{Be} decreases.

Surface roughness has the general effect to increase the sputtering yield at normal incidence and to decrease the yield for large angles of incidence with minimal effects around an angle of incidence of $\alpha = 45°$ [15,16].

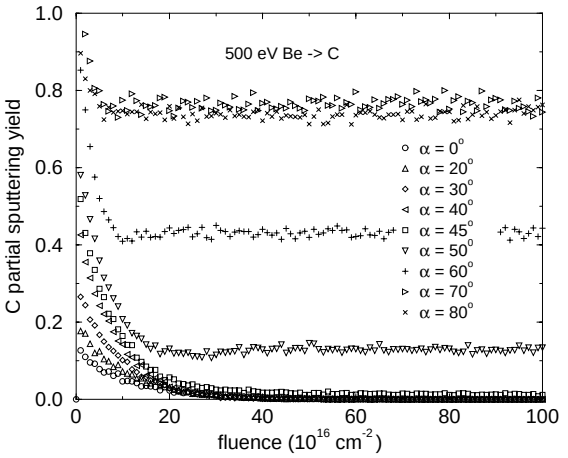

Fig. 4. The C partial sputtering yield versus the incident Be fluence. C is bombarded with 500 eV Be at various angles of incidence, α.

The particle reflection coefficient is lowered in most cases compared to a flat surface. For the bombardment of a rough target surface the results decribed above will certainly be changed, but the general behaviour of erosion and deposition as shown above will persist.

Various results of this kind of calculations performed for different incident energies and various projectile and target species are shown in Fig. 5, where the regions of deposition and erosion are separated by a curve determined from the transition points. In Fig. 5(a) two curves are shown, one for the bombardment of C with Be and one for the bombardment of Be with C. In both cases deposition occurs in the whole energy range given for angles of incidence below about 45°. Towards lower projectile energies erosion is restricted to larger angles of incidence due to the decreasing sputtering yield (with decreasing energy) and increasing reflection. Recalling that at steady-state thick Be layers form on top of the C substrate below some angle of incidence, the border line between erosion and deposition should be given approximately for conditions where $Y_{\text{tot}} + R_N = 1$ for self-bombardment. Calculated values for Y and R_N due to self-bombardment can be found in [17]. Inserting the corresponding values for self-bombardment into Fig. 5 leads to the same transition curve corroborating the interpretation giving above within the limits of interpolation errors. Horizontal and vertical error bars (open symbols) originate from the interpolation of data in the tables of [17]. The lower surface binding energy of Be (3.38 eV) compared to C (7.41 eV) is responsible for the extension of the Be on C curve to lower energies.

A similar plot as in Fig. 5(a) for the Be/C system is shown in Fig. 5(b) for the Be/W system. The curve for Be on W is nearly the same as for Be on C. This is clear from the argument given above, that this curve should be given approximately by the values for Be self-bombardment. The W bombardment of Be shows a different behaviour, a strong decrease down to normal incidence ($\alpha = 0°$). For W bombardment above an energy of 1 keV only erosion occurs for all angles of incidence. The reason is the larger W self-sputtering yield which increases above unity at about 1 keV; the particle reflection coefficient is negligible for normal incidence ($R_N \approx 0.01$). The self-sputtering yields again agree approximately with the W on Be curve. Fig. 5(c) shows the corresponding dependencies for the C/W system, which are very close to the Be/W system. The reason, that the values for self-sputtering [13] agree only approximately with the values calculated in this paper, is the inhomogeneity of the target composition with depth for the curves calculated here compared to the situation of one component target for self-sputtering.

In the deposition case, the deposited film thickness grows proportional with the incident fluence (above some fluence). On the contrary, in the case of erosion, a constant depth profile of the implanted species is

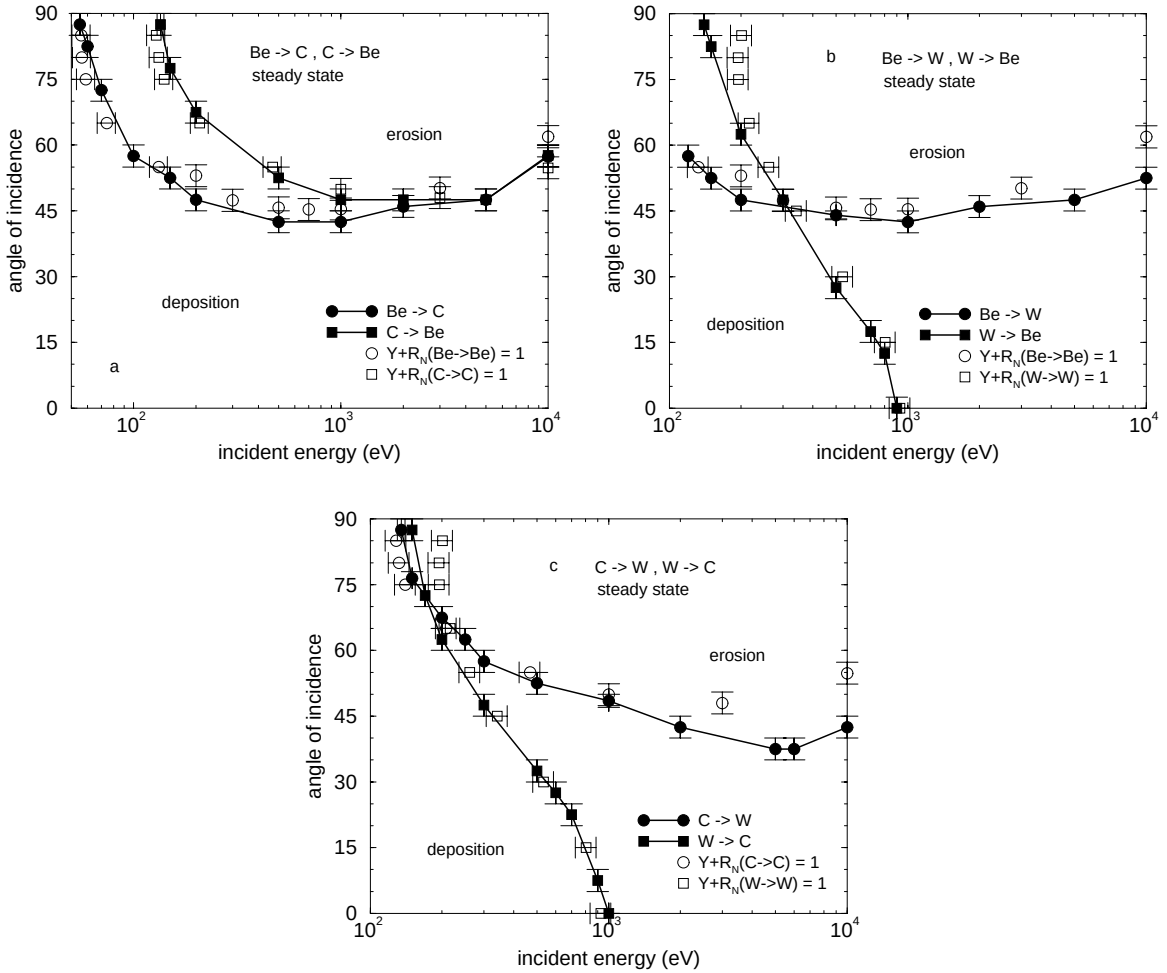

Fig. 5. Regions of deposition and erosion versus the incident energy and incidence angle at steady-state conditions for the bombardment of: (a) C with Be and of Be with C, (b) W with Be and of Be with W and (c) W with C and of C with W. For both examples, the region below each curve belong to the deposition regime, the region above each curve to the erosion regime. Lines drawn to guide the eye.

established at equilibrium. This depth profile depends on the incident energy and the angle of incidence. Examples are shown in Fig. 6 for 500 eV Be on C with the angle of incidence as parameter, and for W on Be at normal incidence in the energy range from 1 to 10 keV, in Fig. 7. The Be profiles become narrower with increasing angle of incidence as expected from the more glancing incidence (lower penetration depth). For the same reason and increasing reflection the maximum concentration decreases with increasing angle of incidence. At a first glance it looks surprising, that at $\alpha = 45°$ a complete Be layer of 3 nm is formed, though it is in an erosion regime. The explanation is a small escape probability of C atoms from depths below 3 nm (see [18]). In the case of W impinging on Be, the profiles become broader with increasing energy due to the larger penetration depth. The maximum concentration decreases with increasing energy; this decrease is faster near 1 keV and becomes small at energies around 10 keV. For energies above 2 keV an increased W concentration in the uppermost layer is observed, see Fig. 7, which has often been found for heavy ion implantation in such kind of calculations. One possible explanation for this finding is the larger escape depth of C atoms compared to W atoms [18].

From the depth distributions at steady-state, like those given in Figs. 6 and 7 for the erosion regime, the maximum atomic fraction of the implanted species at steady-state can be determined. Results are shown in Fig. 8(a) for Be impinging on C, and in Fig. 8(b) for W bombardment of C. Points in the energy versus angle of incidence plane for maximum atomic Be fractions of 0.8, 0.5, and 0.2 are given in Fig. 8(a) for Be bombardment

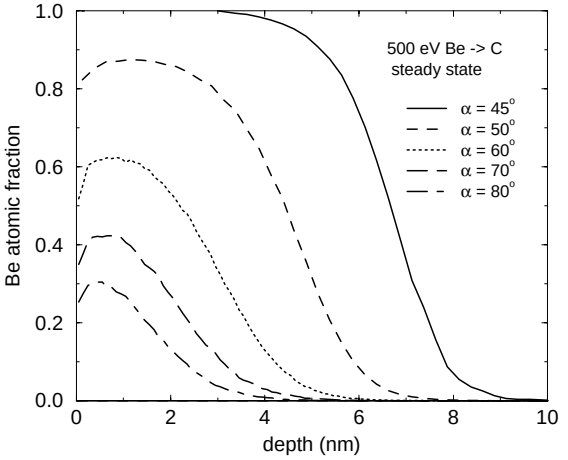

Fig. 6. Depth distributions of implanted Be at steady-state conditions. C is bombarded with 500 eV Be at various angles of incidence, α.

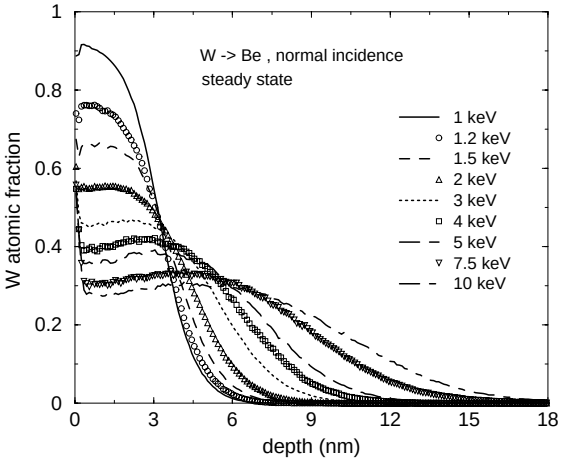

Fig. 7. Depth distributions of implanted W at steady-state conditions. Be is bombarded with W at various energies and normal incidence.

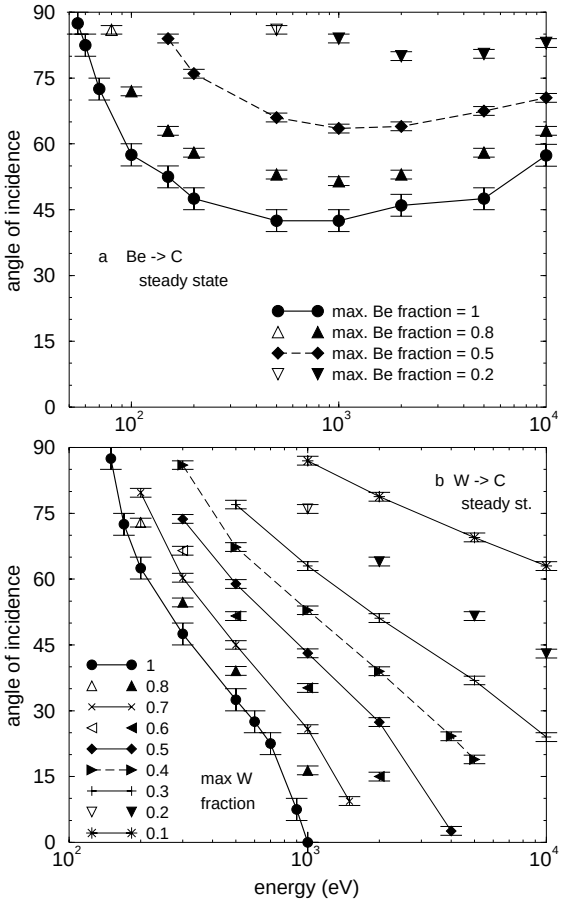

Fig. 8. Points of the maximum atomic fraction of projectile species. The full circles show the maximum projectile fraction of unity (same as in Fig. 5): (a) Be bombardment of C at normal incidence and (b) W bombardment of C at normal incidence. Lines drawn to guide the eye.

of C together with the points separating the erosion and deposition regions (solid line with full circles in Fig. 5(a), which corresponds to a maximum Be fraction of unity). The curves for the given atomic Be fraction are approximately parallel to the curve which separates the deposition from the erosion region (curve for 100% Be coverage). The maximum atomic Be fraction is monotonously decreasing with increasing angle of incidence. Similar curves for the maximum atomic W fraction for the W bombardment of C at steady-state are shown in Fig. 8(b). In the determination of the maximum atomic W fraction the increase of the atomic W fraction at the surface, see Fig. 7, has been neglected. As in the case of Be impinging on C the curves are approximately parallel to the curve of 100% W coverage (solid line with full squares in Fig. 5(c)). With increasing W energy and angle of incidence the maximum W fraction at steady-state decreases. The reason is the increase of the implantation depth and of the sputtering yield with increasing energy and the increase of the particle reflection coefficient and of the sputtering yield with increasing angle of incidence.

Fig. 9 shows the partial sputtering yields at equilibrium for the examples of Be bombardment of C at $\alpha = 60°$ and of W bombardment of C at normal incidence. The partial W sputtering yield is practically unity as it should be at steady-state, whereas the C sputtering yield increases from 0.8 at 300 eV to 0.9 at 10 keV. The reason for this different behaviour is the particle reflection coefficient, which is an order of magnitude larger for the C case ($\approx$0.2 to 0.1) and decreases with increasing energy. The maximum in the C partial yield develops,

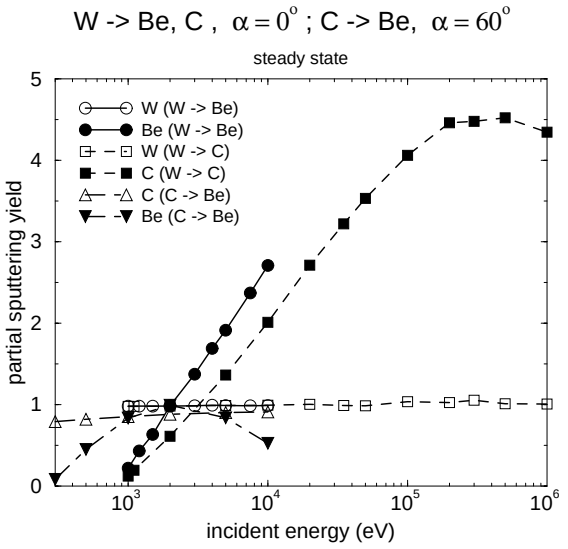

Fig. 9. The partial sputtering yield at steady-state conditions versus the incident energy. Be and C isbombarded with W at normal incidence, and Be is bombarded with C at $\alpha = 60°$. Lines drawn to guide the eye.

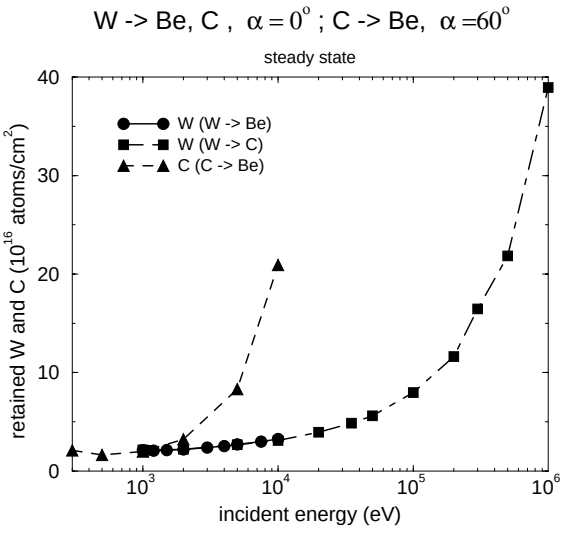

Fig. 10. The retained amount of implanted species at steady-state conditions versus the incident energy. Be and C is bombarded with W at normal incidence, and Be is bombarded with C at $\alpha = 60°$. Lines drawn to guide the eye.

because the maximum yield for self-bombardment of Be and C at $\alpha = 60°$ is in the low kilo-electron-volt range, and the fraction of Be at the surface at equilibrium has a maximum at about 2 keV. The Be and C partial yields due to W bombardment both increase with the incident energy, whereas the Be yield increase is somewhat faster than the C yield increase due to the lower surface binding energy of Be. The W partial yield exhibits a maximum at about 300 keV. It should be remembered that the composition profile at equilibrium changes with the incident energy.

Besides the depth distribution of implanted species the retained amount can be measured. The retained W and C for the same examples as above is shown in Fig. 10. The retained C in the Be target is larger than the retained W at the same energy. Whereas the retained W increases only by about 50% from 1 to 10 keV, the retained C increases by about an order of magnitude in the same energy range. The reason is the larger range of C than that of W. The strongest increase in the retained W occurs for energies above 100 keV.

4. Conclusions

Computer simulations with the dynamic Monte Carlo program TRIDYN have shown that, dependent on the incident energy and on the angle of incidence, ion bombardment of solids results in regions of erosion and deposition. This was demonstrated for the systems Be on C, C on Be, Be on W, W on Be, C on W, and W on C in the energy range from 100 eV to 10 keV, in some cases up to 1 MeV. The separation of the erosion and deposition regimes can be approximately given by the condition, that the 'sum of the partial sputtering yields and the particle reflection coefficient is equal to unity' for self-bombardment. Depth profiles of the implanted species at equilibrium are given for two examples, 500 eV Be bombardment of C and W bombardment of Be at normal incidence, in the erosion case, where constant depth profiles are established.

The steady-state behaviour of the energy dependence of the sputtering yield, the mean range, and the retained amount of implanted atoms is compared for three erosion cases, W on Be and C at normal incidence and C on Be at 60°. For W bombardment at normal incidence the Be and C partial sputtering yields increase with increasing energy. In the case of the C target the calculations have been extended up to 1 MeV, and the partial C yield exhibits a maximum at about 300 keV. The Be yield has a maximum at about 2 keV for C bombardment of Be at $\alpha = 60°$. The mean range and the retained amount of C is larger than the retained amount of W, above 1 keV, and this difference is increasing with incident energy up to 10 keV.

The systems investigated show a complex behaviour, which indicate that the use of different wall materials in the same fusion machine will result in a complex composition of the plasma facing surface, which is difficult to predict in detail.

Acknowledgements

The author acknowledges greatly many helpful discussions with J. Roth and R. Bastasz and the hospitality of Sandia National Laboratories, Livermore.

References

[1] ITER Physics Expert Group on Divertor, ITER Physics Expert Group on Divertor Modelling and Database, ITER Physics Basis Editors, ITER EDA, Nucl. Fusion 39 (12) (1999) 2391ff (Chaper 4).
[2] K. Krieger, H. Maier, R. Neu, the ASDEX Upgrade-team, J. Nucl. Mater. 266–269 (1999) 207.
[3] H. Maier, K. Krieger, M. Balden, J. Roth, the ASDEX Upgrade-team, J. Nucl. Mater. 266–269 (1999) 1003.
[4] M. Rubel, V. Philipps, A. Huber, T. Tanabe, Phys. Scr. T 81 (1999) 61.
[5] W. Eckstein, J. Roth, Nucl. Instrum. and Meth. B 53 (1991) 279.
[6] W. Eckstein, J. Roth, E. Gauthier, J. László, Fusion Technol. 19 (1991) 2076.
[7] W. Möller, W. Eckstein, J.P. Biersack, Comp. Phys. Commun. 51 (1988) 355.
[8] W. Eckstein, Computer Simulation of Ion–Solid Interaction, Springer, Berlin, 1991.
[9] J.P. Biersack, W. Eckstein, Appl. Phys. A 34 (1984) 73.
[10] W.D. Wilson, L.G. Haggmark, J.P. Biersack, Phys. Rev. B 15 (1977) 2458.
[11] J. Lindhard, M. Scharff, Phys. Rev. 124 (1961) 128.
[12] O.S. Oen, M.T. Robinson, Nucl. Instrum. and Meth. 132 (1976) 647.
[13] W. Eckstein, M. Hou, V.I. Shulga, Nucl. Instrum. and Meth. B 119 (1996) 477.
[14] W. Eckstein, V.I. Shulga, J. Roth, Nucl. Instrum. and Meth. B 153 (1999) 415.
[15] M. Küstner, W. Eckstein, V. Dose, J. Roth, Nucl. Instrum. and Meth. B 145 (1998) 320.
[16] M. Küstner, W. Eckstein, E. Hechtl, J. Roth, J. Nucl. Mater. 265 (1999) 22.
[17] W. Eckstein, IPP-Report 9/117, Garching, 1998.
[18] W. Eckstein, V.I. Shulga, Nucl. Instrum. and Meth. B 164&165 (2000) 748.